Full 3D Touchless Fingerprint Recognition: Sensor, Database and Baseline Performance

Javier Galbally, Gunnar Bostrom and Laurent Beslay
European Commission, DG Joint Research Center (DG-JRC), ITALY
{javier.galbally, gunnar.bostrom, laurent.beslay}@ec.europa.eu

Abstract

One of the fields that still today remains largely unexplored in biometrics is 3D fingerprint recognition. This gap is mainly explained by the lack of scanners capable of acquiring on a touchless, fast, reliable and repeatable way, accurate fingerprint 3D spatial models. As such, full 3D fingerprint data with which to produce research and advance this field is almost nonexistent. If such acquisition process was possible, it could represent the beginning of a real paradigm shift in the way fingerprint recognition is performed. The present paper is a first promising step to address the fascinating challenge of 3D fingerprint acquisition and recognition. It presents a new full 3D touchless fingerprint scanner, a new database with 1,000 3D fingerprint models, a new segmentation method based on the additional spatial information provided by the models, and initial baseline verification results.

1. Introduction

There is an intrinsic inconsistency between the physiology of fingerprints and the way in which fingerprint recognition works. Human fingerprints are 3D anatomical structures that, in their natural state, are not deformed by contact with an object. However, in contrast, the vast majority of fingerprint recognition systems are based on 2D images acquired through the contact of the fingerprint with a surface that introduces a certain level of distortion very difficult to quantify.

In spite of this inconsistency, over years of constant development from the first pioneering works, automatic 2D touch-based fingerprint recognition has proven to work. And to work well. However, it should not be overlooked that the inconsistency remains at the core of the technology: the samples used to perform the authentication process.

The key question is: What is the potential improvement of fingerprint recognition technology if such inconsistency was overcome? That is, if instead of using as input samples 2D pixel-based images acquired while the fingerprint is physically deformed, fingerprint systems relied on spatial 3D models captured in a touchless manner. In such hypothetical scenario, a real breakthrough in the accuracy of the technology could be expected thanks to the additional information available in 3D models.

The fact is that, capturing a *high-quality* 3D model of a fingerprint is a very challenging task. Up to date, in spite of some recent valuable initiatives (see Sect. 2), there has not been yet any sensor proposal that is able to accomplish the feat with sufficient degree of detail, in a fast, consistent and repeatable way. As a result, full 3D fingerprint recognition is still a theoretical exercise with no real database to back it up. In the meanwhile, 2D-touch-based sensors keep to produce more reliable representations of fingerprints and higher accuracy recognition results.

The present paper is a first promising step to address the fascinating challenge of 3D fingerprint acquisition and recognition. Its contributions can be summarized as follows: 1) Development of the first sensor based on laser sensing technology capable of acquiring accurate fingerprint 3D models in a touchless manner; 2) Presentation of the first database of 3D fingerprints, comprising 200 different identities; 3) Development of a new fingerprint segmentation method for 3D finger models based on the fingerprint curvature; 4) Baseline accuracy results for full 3D fingerprint verification.

The rest of the article is structured as follows. Sect. 2 gives a quick overview of the most relevant related works. The touchless 3D acquisition sensor is described in Sect. 3. The new acquired 3D fingerprint database is presented in Sect. 4, while a novel segmentation method and initial verification results are given in Sects. 5 and 6 respectively. Conclusions are finally drawn in Sect. 7.

2. Related Works

In the current state of the art in fingerprint recognition, we can find some research works and also industrial applications that have advanced, to some extent, in the direction

978-1-5386-1124-1/17/$31.00 ©2017 IEEE

proposed by this work.

Over the last few years, several laboratories and leading biometric companies have proposed specific sensors for the acquisition of 2D fingerprint images in a touchless mode. These methods are in different development phases ranging from R&D, to full finalized commercial scanners [23, 2, 21, 25]. Also in recent times, several works have started to address the problem of touchless 2D fingerprint acquisition and recognition using photo cameras, especially in the context of smartphones [24, 14, 18, 28]

The reader should be aware that some of the on-going touchless projects announce the acquisition of 3D fingerprints. However, these works are based on capturing one or multiple *2D pixel-based images* of the finger, from one or different angles. None of them considers the direct acquisition of a full 3D fingerprint model consisting of vertices defined by its (x, y, z) spatial coordinates. In those works, the 2D images are used to: 1) reconstruct a single 2D pixel-based fingerprint image "tip-to-tip", similar to the "rolled fingerprint images" obtained through the traditional inking method [9, 29, 25]; 2) reconstruct a 3D model of the fingerprint, using different *estimation* methods from several 2D images [17, 15, 7, 8]; 3) synthetic digital 3D models estimated from a single standard 2D image, which can even be used to generate physical 3D gummy finger phantoms [4, 3, 16].

Although this "estimate and reconstruct" formula has had some success, it is not able to tackle the spatial information loss derived from the initial acquisition of 2D images to generate a final 3D point cloud.

Another recent on-going research line that mentions the acquisition of 3D fingerprints studies the potential of the Full-Field Optical Coherence Tomography (FF-OCT). This is an imaging technology used in medicine capable of acquiring not only the fingerprint surface but also features coming from internal skin layers [5, 11, 10]. The scanner captures, in a touchless manner, 2D images of the transversal section of the skin. This way, the spatial z dimension can be approximated from the successive finger "slices". As in the works mentioned above, the final 3D point cloud is estimated from the set of 2D images and not directly acquired by the scanner.

From the different initiatives found in the literature dealing with the acquisition of 3D fingerprints, probably the one which is closest to the method proposed in the present work was first described in [13]. The scanning device used in that work is based on structured light illumination (SLI). Structured-light 3D scanners project a pattern of light on the target and look at the deformation of the pattern on the subject. The pattern is projected onto the subject using a stable light source. A camera, offset slightly from the pattern projector, looks at the shape of the pattern and calculates the distance of every point in the field of view according to its deformation. The three main challenges of SLI technology for 3D fingerprint scanning are: 1) SLI-based scanners very often encounter difficulties handling translucent materials, such as skin and human tissue because of the phenomenon of sub-surface scattering; 2) the resolution of SLI-based scanners is not yet at the level of triangulation-based scanners such as the one used in the present work (see Sect. 3). Not sufficient spatial accuracy can result in very noisy samples for such detailed structures as fingerprints. Initial results were presented in 2010 using a SLI-based scanner to capture a database of 11 users and 441 3D fingerprint samples [27, 26]. However, no further improvements or developments have been published since that date.

3. Touchless Full 3D Fingerprint Acquisition

Fingerprint ridges are very fine physical structures with a size in the range of 0.1-0.3 millimeters [20]. Acquiring an accurate 3D model of such small dimension constitutes a real engineering challenge. The task becomes even more difficult considering that a finger is a living object that cannot be kept fully still.

From the different 3D scanning technologies available in the market, non-contact 3D active scanners based on triangulation present the highest accuracy which can get down the range of a few microns making them a perfect fit for the acquisition of fingerprints. Their main drawback is that they have a quite limited range of operation (i.e., distance between the target and the sensor), which can be limited to only several centimeters if very high resolution is required. However, this is not a special limitation for the specific case of 3D fingerprint scanning, as the finger can be placed as close to the sensor as needed.

Following the above discussion, the 3D fingerprint scanning device developed for the present work (shown in Fig. 1) is a non-contact active scanner based on the triangulation principle. The scanner uses an active light, in this particular case a line projection laser diode, to illuminate the target (i.e., finger). A fast industrial CMOS camera captures from an angle with respect to the laser diode, the reflected light on the target. This way, the shape of the imaged line on the sensor can be directly related to the shape of the target along the laser line through triangulation.

This technique is called triangulation because the laser line, the camera and the laser diode form a triangle (as shown in panel (e) of Fig. 1). The length of one side of the triangle L, the distance between the camera and the laser diode is known. The angle of the laser emitter corner is also known (perpendicular to the ground). The angle of the camera with respect to the ground is also known, in this case 45°. This way, the angle of the observed object can be determined by looking at the location of the laser line in the camera's field of view. These three pieces of information (i.e., length of the side L, angle of the laser diode and angle

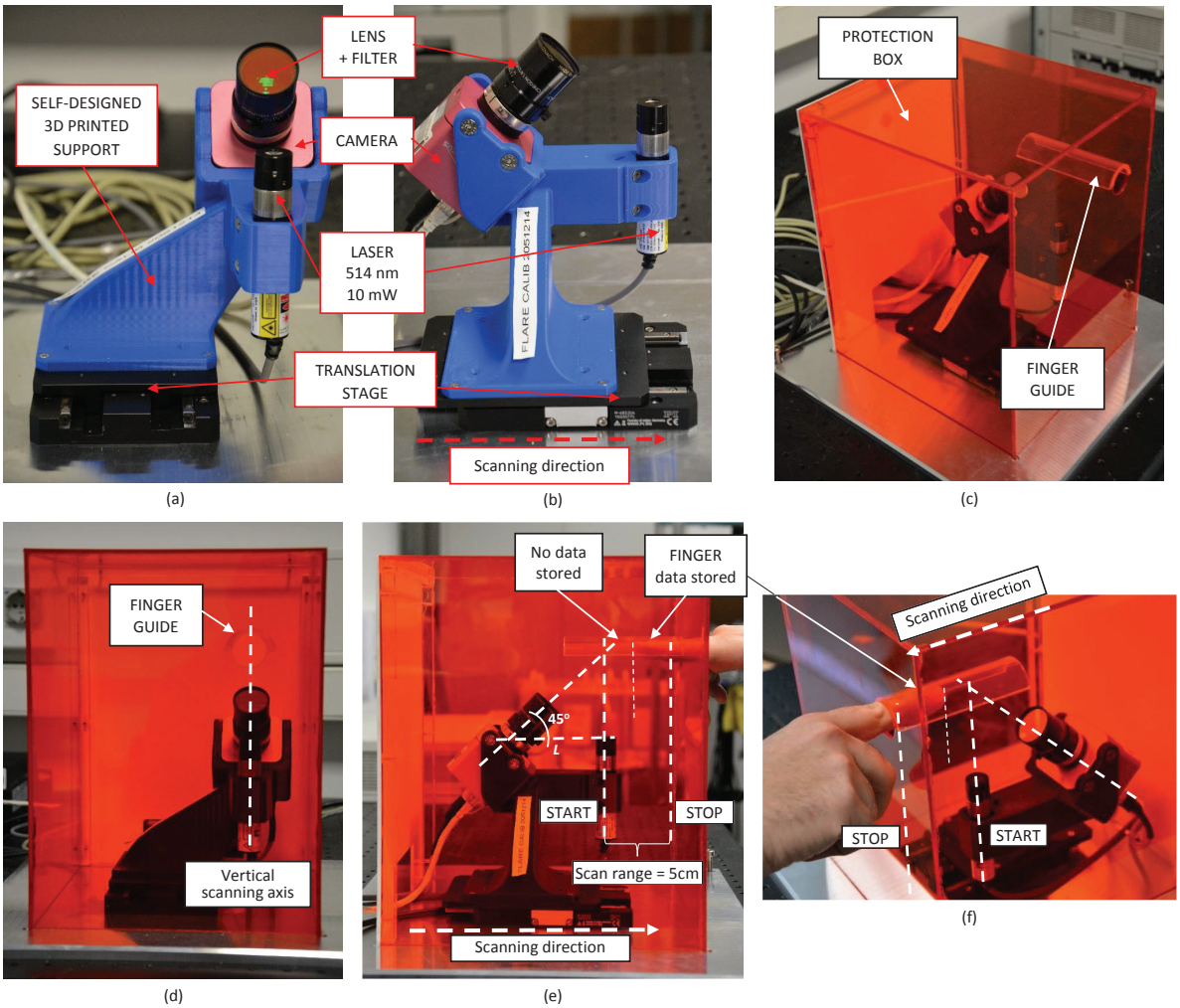

Figure 1. Pictures of the 3D fingerprint sensor.

of the observed object) fully determine the shape and size of the triangle and give the location of the target segment illuminated by the laser line.

As shown in the three pictures of the top row in Fig. 1, the 3D fingerprint scanning prototype assembled for this research is composed of:

- *Laser diode*. The human skin optical characteristics changes with light wavelength. For longer wavelength in the visual spectra, i.e. red to deep red colors (650nm), the skin has a tendency not just to reflect but also to transmit into the tissue. This means that an illuminated spot is observed not just by the directly reflected light but also a glowing area around the illumination. This is caused by the light transmitted into the tissue which reflects parts of its light after being internally refracted in deeper layers. This translates into quite inaccurate readings of the skin surface. For shorter wavelength, i.e. green-blue, this tendency decreases. With this in mind, an active light with shorter wavelength is favorable. As such, a 514nm StingRay Laser Diode (10mW) emitting green light was selected.

- *Camera*. The fingerprint scanning prototype uses an industrial 3D enabled camera manufactured by PhotonFocus. The CMOS sensor in the camera presents a resolution of 2048×1088 pixels and is connected internally with high-speed electronics which compute the position of the laser projected line along the sensor through the triangulation process described above.

- *Optics*. The imaging system used by the camera consists of a high quality lens with a focal length of 12mm and a band-pass filter matching the active 514nm wavelength of the laser in order to optimize the signal-to-noise ratio.

- *Fixing support*. Both the camera and the laser diode

are mounted to a blue plastic fixing arm designed and produced (3D printed) in our lab (see pictures (a) and (b) in Fig. 1). The support holds the laser and the camera so that the angle between the scanning illumination axis and the optical axis is 45°(see pictures (d) and (e) in Fig. 1).

The key optimization parameter for the scanning prototype is the accuracy of *absolute* 3D positioning. For this purpose, the complete set, including camera and laser mounted on the fixing support, is calibrated so that each pixel on the CMOS sensor represents an absolute position along the laser-projected plane.

- *Translation stage + motor controller*. The translation stage moves the fixed support holding the laser diode and the camera at a constant speed in order to scan the fingerprint. The movement is handled by a motor controller that receives commands from the acquisition software.

  The translation stage presents a maximum scanning range of 5 cm from the starting to the finishing position (as shown in picture (e) of Fig. 1). This way, in order to acquire the full fingerprint, from the tip to the joint of the 3rd phalange, the finger has to be inserted less than 5 cm. Typically, in order to avoid acquisition errors, only the 2nd and 3rd phalanges should be inserted through the whole in the protection filtering box.

  The stage can vary his speed up to 50 mm/sec (covering its whole range in just one second).

- *Protection box*. The outside orange box that can be seen in the bottom row of Fig. 1, was designed and built specifically for the project in our lab. It fulfills two main goals: 1) serve as safety measure for the laser diode. The box is made of plexiglass panels that absorb the light emitted by the laser (the same as specific laser protection glasses or goggles). It should be noted that the laser is in the very low range of laser class IIIb for which protection goggles are only *suggested* (neither recommended nor mandatory). 2) Serve as a guide for the placement of the fingerprint both in height and direction (see pictures (e) and (f) in Fig. 1). In order to get an accurate 3D reconstruction it is important that the finger is placed approximately at the height where the laser and camera axis intersect (please see the middle picture of the bottom row in Fig. 1). This way, it is guaranteed that the projected laser line falls within the sensor field of view when it illuminates the target.

  This guide to place the finger limits the amount of misalignment among samples. Roughly, all fingers are captured facing down, perpendicular to the laser, along the direction of the movement of the translation stage. Accordingly, the acquisition process helps to simplify the necessary segmentation and alignment steps prior to the matching.

- *Acquisition software*. A specific software application was developed in order to: 1) select and regulate the scanning speed; 2) automatically control the sequence followed for the generation of the 3D-FLARE DB in order to minimize acquisition mistakes (please see Sect. 4 for further details on the DB); 3) automatically store the captured files with the correct naming convention.

  The software controlling the acquisition sensor only stores data in the section of the 5cm scanning range where it detects the presence of an object (i.e., finger). Accordingly, during the acquisition, no data is stored until the fingertip is reached (see pictures (e) and (f) in Fig. 1).

The sensor produces files in PLY format. In these files the finger is represented by a $N \times 3$ matrix, where each of the N rows is a point defined by its spatial coordinates $[x, y, z]$ (columns in the matrix). The resolution in the x dimension (transversal to the finger) is approximately 0.03mm. The sensor moves longitudinally to the fingerprint along the y dimension. As such, this spatial resolution depends on the scanning speed and the sampling rate of the camera. At the configuration used to acquire the database that will be described in Sect. 6 (i.e., 50mm/sec scanning speed and 600 frames/sec), the resolution in the y dimension is approximately 0.08mm. The depth resolution in the z direction given by the camera manufacturer is up to 0.006mm. With this speed/frame-rate configuration, the resulting files weigh approximately 3-5 Mbytes (depending on the size of the finger), being each sample defined by around $N = [100 \cdot 10^5, 200 \cdot 10^5]$ points.

The previous resolutions in each of the axes are theoretical optimal values that can be obtained when scanning perfectly still objects. However, it is not possible to maintain a finger absolutely motionless. In order to cope with this limited motion, the software in charge of computing the absolute spatial values of the final point cloud assumes that the target presents a smooth surface with no discontinuities (as is the case for a finger). Whether or not the sensor is capable of suppressing the finger movement in order to produce an accurate enough 3D model can only be determined through testing. Section 4 describes the database acquired and the baseline 3D fingerprint recognition system developed in order to initially assess the capabilities of the developed acquisition scanner.

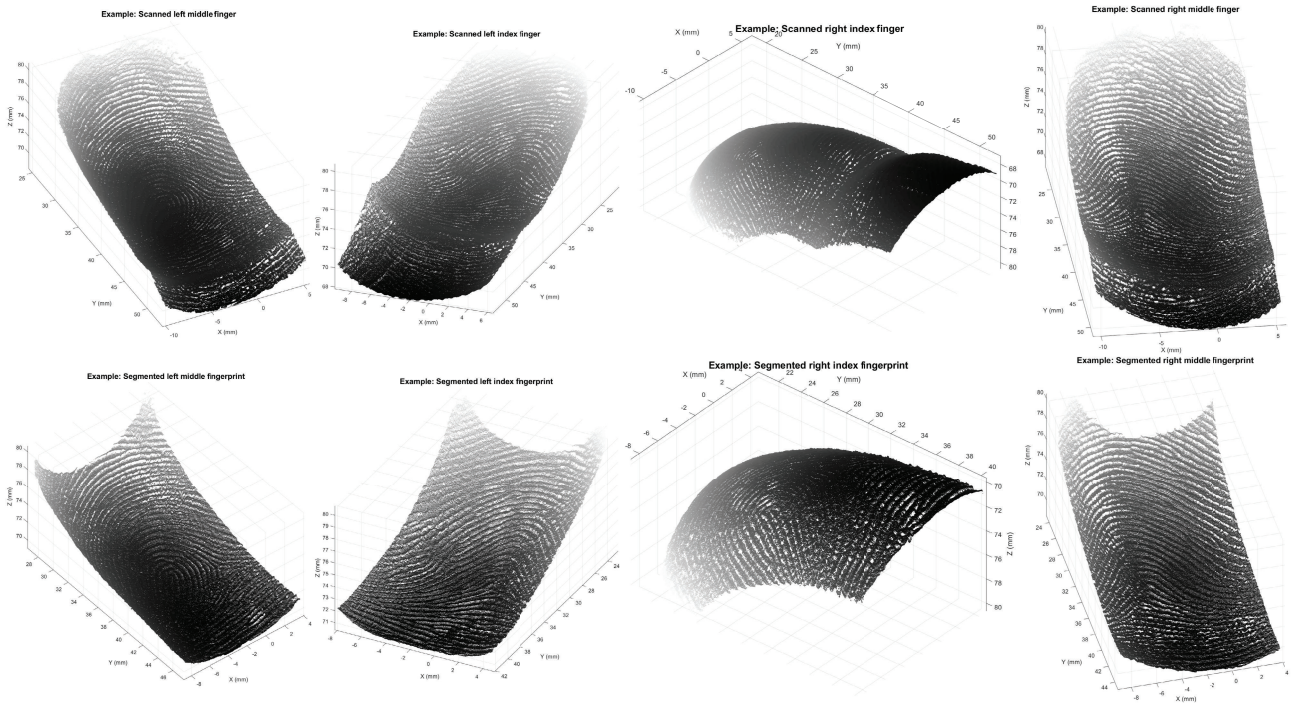

Figure 2. First row: Examples of the four fingers acquired for the database, from left to right: left middle, left index, right index and right middle. Second row: Segmented fingerprints for the fingers in the first row, following the method described in Sect. 5. Each sample is represented from a different view point in order to better illustrate the 3D nature of the models.

4. 3D Fingerprint LAser REcognition Database: 3D-FLARE DB

In order to test the soundness and consistency of the developed 3D scanning sensor a new database was acquired. The 3D Fingerprint LAser Recognition DB (3D-FLARE DB) contains the index and middle finger of both hands from 50 users, that is, 200 different fingers. All users are Caucasian adults between 28 and 55 years of age, computer-based workers, with a gender ratio of 40 men and 10 women. The acquisition was conducted in a standard office-like environment with no specific control over illumination. Users were given the option to be sitting on a revolving chair in front of the sensor or standing up, depending on what position felt more comfortable for them.

Each finger was acquired 5 times at a speed of 50 mm/sec (fastest speed allowed by the translation stage). The camera was configured at a rate of 600 frames/sec. In order to have a more realistic acquisition scenario, samples of the same finger were not acquired consecutively. The scanning sequence followed by the user five times was: left middle, left index, right index and right middle. This way, for each acquisition, the user had to remove the finger and introduce the next one in the sequence. This process ensures to have a sufficient variability among samples from the same finger. The acquisition of all 20 samples (4 fingers $\times$ 5 samples) of the same user was done in around 2 minutes. In order to minimize mistakes during acquisition, a specific application was developed to automatically control the acquisition and file storage processes.

Four examples of the typical 3D fingerprint models that can be found in the database are shown in the first row of Fig. 2. All four fingers correspond to the same user. Different view points have been used for each of the samples in order to better illustrate the three dimensional nature of the models.

In order to have an initial estimation of the discriminative power of the acquired 3D fingerprint models, a simple verification system was developed with which to obtain baseline accuracy results. The system is composed of two different modules: 1) segmentation: the fingerprint Region of Interest (ROI) is extracted from the whole scanned finger; 2) matching: compares two segmented fingerprints. The system and results are described in the following sections.

5. 3D Fingerprint Segmentation Based on the Finger Curvature

The raw data captured by the 3D sensor corresponds to the whole length of the finger inserted within the scanning range. This raw model typically includes part of the second phalange as shown in the top row of Fig. 2. Therefore, sim-

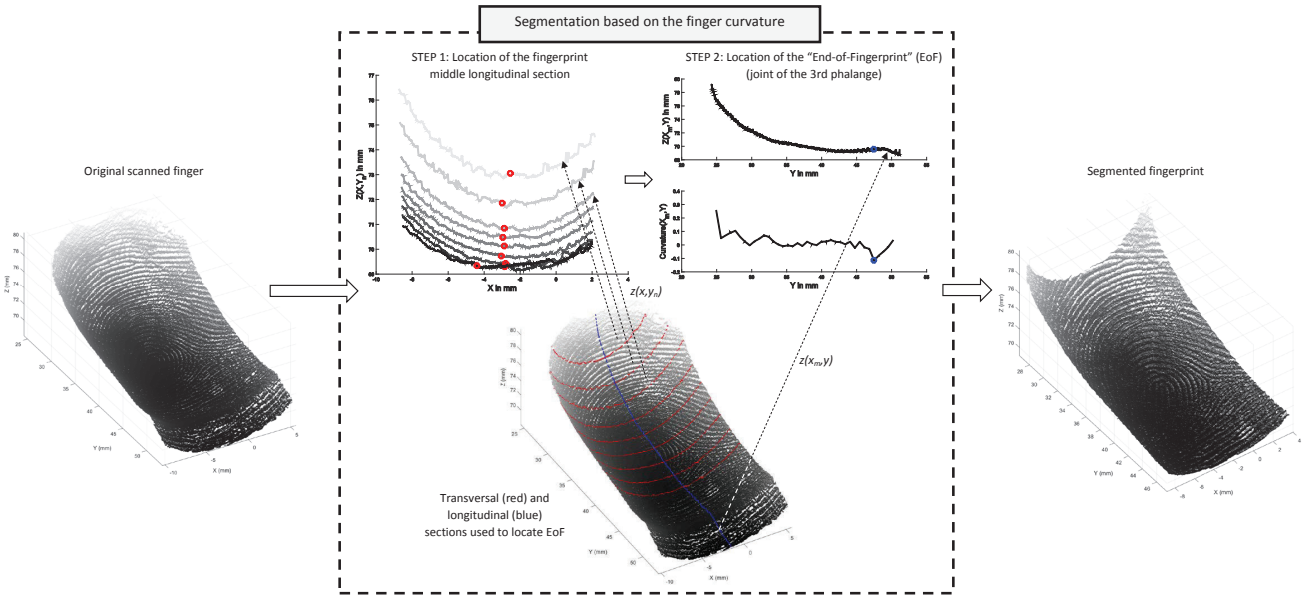

Figure 3. Fingerprint segmentation method based on the curvature of the fingerprint described in Sect. 5.

ilarly to what is done in 2D fingerprint recognition, the first step is to select the "Region of Interest" (ROI), that is, the part of the acquired model corresponding to the fingerprint (i.e., third phalange).

The novel segmentation method described in this section takes advantage of the extra information present in 3D models with respect to 2D images in order to find to ROI. In particular, it is based on the curvature of the finger, a feature which cannot be obtained from the flat representations of the fingerprint (i.e., pixel-based pictures) used in traditional 2D systems.

As any 3D object, a 3D finger model can be seen as a function $z(x, y)$. The ROI will be defined by a rectangle $[x_{min}, x_{max}]$ and $[y_{min}, y_{max}]$ that contains the z info corresponding only to the fingerprint. The objective of the segmentation process will be to find those four limits.

Limits in the y axis (i.e., longitudinal to the fingerprint). The key of the whole segmentation process is to find y_{max}. This will be referred to as the "End-of-Fingerprint" point (EoF) and will be defined as the joint of the 3rd phalange of the finger. Once that point is located, the other three limits (i.e., y_{min}, x_{min} and x_{max}) will be defined from it.

In order to locate the EoF, two successive steps are followed (depicted inside the dashed square in Fig. 3).

- *Step 1: Location of the middle longitudinal section of the fingerprint*(i.e., "middle" in the direction of the x axis). This step is plotted in the top left panel of Fig. 3. Nine equidistant transversal sections (i.e., in the direction of the x axis) of the finger are taken starting from the fingertip along the y axis. These sections correspond to $z(x, y_n)$, where y_n are the different nine sampling points along the y axis, with $n = 1, \ldots, 9$ (plotted in red in the bottom panel of Fig. 3). All sections are smoothed using a 30 point moving average filter. The minimum of the smoothed sections (shown with red circles in Fig.3 left panel) is selected as the middle of the finger for that particular point y_n of the longitudinal axis y. The final value of the middle longitudinal section (in blue in the bottom panel of Fig. 3) is computed as the average of the nine middle points of the transversal sections and will be noted as x_m.

- *Step 2: Location of the "End-of-Fingerprint" point.* Depicted in the top right panel of Fig. 3. Once the middle longitudinal section $z(x_m, y)$ has been located in Step 1, it is smoothed using a 40 point moving average filter. The resulting smoothed section is downsampled in order to take only 40 equidistant points including the first and last. This smoothed, downsampled signal will be referred to as $z_{sd}(x_m, y)$. In order to obtain its curvature, the second derivative with respect to the y dimension is computed, that is, $curvature(x_m, y) = d^2(z_{sd}(x_m, y))/d(y)^2$. The "End-of-Fingerprint" point $z(x_m, y_{EoF})$, plotted in blue in the top right panel of Fig. 3, coincides with the minimum of this curvature signal.

Once the limit y_{max}, i.e., EoF, has been set, the limit y_{min} is defined as $y_{min} = 0.1L$, where L is the length of the fingerprint between the fingertip (first scanned point in the longitudinal axis) and EoF. The fingertip is not taken as the initial point of the fingerprint because, towards the edges, the laser illuminates the finger with an angle that di-

verges significantly from the perpendicular, losing spatial accuracy.

Limits in the x axis (i.e., transversal to the fingerprint). The x_{min} and x_{max} limits will be close to the sides of the fingerprint. For the same reason as the fingertip is not taken as y_{min}, the absolute maximum and minimum values in x are not taken as the sensor loses accuracy towards the edges of the finger. Consequently we define: $x_{min} = 0.1W$, while $x_{max} = 0.9W$, where W is the maximum width of the scanned finger within the limits $[y_{min}, y_{max} = \mathrm{EoF}]$. This way, around 80% of the scanned finger surface along the x axis is considered.

Some examples of segmented fingerprints following the method described above are shown in the bottom row of Fig. 2.

6. 3D Fingerprint Verification Results

Once the ROI (i.e., fingerprint) has been extracted from the scanned raw finger 3D data according to the method described in Sect. 5, fingerprints are compared according to the Iterative Closest Point (ICP) algorithm. This is a well-established technique used for rigid registration of 3D surfaces, largely studied in the fields of robotics and computer vision [6, 22]. In order to minimize the distance between two cloud points (which is the sum of distances calculated for all points in one of the surfaces, finding the closest point on the other), ICP computes and revises the translation and rotation iteratively. This registration is used to establish point-to-point correspondences between two 3D models. The ICP algorithm was one of the first approaches used in 3D face recognition [1, 19] and, as of today, it is still used as a good baseline method with which to compare more advanced matching techniques [12].

The reader should be aware that two limitations of the ICP-based approach are: 1) as any gradient descent method, it needs a good initialization for an accurate alignment result between the two models and 2) it does not consider non-rigid transformations (i.e., different from translation and rotation), which is required in the presence of surface deformations, such as those that occur in touch-based fingerprint scanners. In the particular case of the present study, such two challenges are addressed thanks to the design of the new acquisition sensor: 1) the finger guide limits the misalignment of fingerprints and 2) since the acquisition process is touchless the possible elastic deformations are minimal, if any.

One of the main outputs of the ICP algorithm is the final minimized distance between the two aligned point clouds which, in our particular implementation, is computed as the root mean square error (RMSE) of the Euclidean distance between each point in point cloud A and its corresponding closest point in point cloud B. In order to have a similarity measure (and not a distance measure), the final matching score s used by the system is $s = 1/\mathrm{RMSE}$.

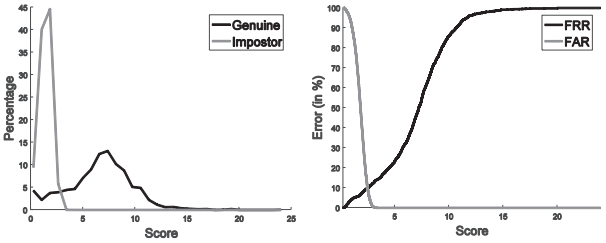

Figure 4. Left: genuine and impostor scores computed according to the protocol described in Sect. 6. Right: False Acceptance Rate (FAR) and False Rejection Rate (FRR) curves derived from the genuine and impostor scores. The Equal Error Rate (EER) is 9.91.

The ICP algorithm was used to obtain baseline 3D fingerprint verification results in the 3D-FLARE segmented DB. For this purpose, two sets of scores were computed: 1) *Genuine scores*, resulting from the comparison of two samples of the same finger and 2) *impostor scores*, resulting from the comparison of two samples from different fingers. Genuine scores were computed matching all 5 samples of the same finger among themselves avoiding duplicated matches (i.e., if sample A has already been matched to sample B, then sample B is not matched to sample A). This method produces 10 scores for each finger. As such, given that there are 200 different fingers in the database the total number of genuine scores computed is $200 \times 10 = 2,000$. On the other hand, impostor scores were computed matching each of the 5 samples of one finger with 5 random samples taken from the rest of users in the DB. Therefore, there are a total $200 \times 5 \times 5 = 5,000$ impostor scores.

The genuine and impostor scores distributions are shown on the left panel of Fig. 4. The resulting False Acceptance Rate (FAR) and False Rejection Rate curves obtained from these two sets of scores are plotted on the right panel, being the Equal Error Rate (EER) of the system EER=9.91.

Given the limitations of ICP as a matching technique, especially for objects with such fine structures as fingerprints, we believe that this initial result is a good proof of the consistency and accuracy of the 3D acquisition scanner developed in the work.

7. Conclusions

Computer-based automatic biometric technology has covered a long path since the first pioneering works in the early 1970s. This is particularly true for the most studied and deployed biometric trait: fingerprints. Such a path of technological evolution has lead to a point in which the biometric community has started to sense that traditional 2D image-based fingerprint recognition is reaching its potential limits for accuracy. These limits have proven to be certainly high, however, in order to get beyond them, a deep redesign

of how fingerprint recognition has been traditionally performed may be needed.

The current article has presented a first step in this direction, showing that a paradigm shift in fingerprint recognition from the 2D plane to the 3D space can be feasible. The paper can be considered as a starting point in the ambitious path of developing 3D fingerprint recognition as a field of research of its own within biometrics, similar to what happened with the appearance of 3D face recognition as a plausible alternative to traditional authentication based on facial pictures.

Even though this is still a novel on-going research line, the work carried out so far has already reached some relevant achievements presented in this paper: 1) It has been shown that it is possible to acquire accurate 3D fingerprint models in a fast and reliable way based on laser sensing technology; 2) A new database for 3D fingerprint recognition has been acquired; 3) It is possible to perform fingerprint segmentation with a high level of precision taking advantage of the spatial information provided by 3D models with respect to 2D images (i.e., curvature of the fingerprint); 4) It has been shown that, even using a fairly simple matching strategy, it is possible to perform 1-to-1 fingerprint verification with a reasonable level of accuracy.

The work also opens many research possibilities to the biometric community that will need to be addressed in the future. Just to mention a few: 1) Study the impact that speed acquisition (i.e., speed of the translation stage integrated in the scanner) has on verification accuracy; 2) Although the ICP algorithm has been used in the past in the field of biometrics for the matching of 3D point clouds with relatively good results, initially it was conceived as an alignment algorithm. Therefore, much improved accuracy is expected by: using ICP as an alignment step after segmentation and prior to a specific and more efficient matching algorithm for 3D fingerprints (e.g., based on minutiae). 3) In the field of fingerprint recognition there are already many databases used for instance in the context of law-enforcement investigations which contain 2D images. As such, the new 3D fingerprint technology should be made compatible with that existing data; 4) Development of quality metrics for the 3D fingerprint models; 5) Spoofing and vulnerability studies.

References

[1] B. B. Amor, M. Ardabilian, and L. Chen. New experiments on ICP-based 3D face recognition and authentication. In *Proc. of Intl. Conf. on Pattern Recognition (ICPR)*, page 11951199, 2006.

[2] ANDIOTG. Andiotg scanner. Online, 2016. `www.andiotg.com/`.

[3] S. S. Arora, K. Cao, A. K. Jain, and N. G. Paulter. 3D fingerprint phantoms. In *Proc. Intl. Conf. on Pattern Recognition (ICPR)*, 2014.

[4] S. S. Arora, K. Cao, A. K. Jain, and N. G. Paulter. Design and fabrication of 3D fingerprint targets. *IEEE Trans. on Information Forensics and Security*, 2016.

[5] E. Auksorius and A. C. Boccara. Fingerprint imaging from the inside of a finger with full-field optical coherence tomography. *Biomedical Optics Express*, 6, 2015.

[6] P. J. Besl and N. D. McKay. Method for registration of 3-D shapes. *IEEE Trans. on PAMI*, 14:239–256, 1992.

[7] D. Boyanapally. Merging of fingerprint scans obtained from multiple cameras in 3D fingerprint scanner system. Master's thesis, University of Kentucky, 2008.

[8] Y. Chen, F. Han, H. Liu, and J. Lu. 3D reconstruction from planar points: A candidate method for authentication of fingerprint images captured by mobile devices. In *Proc. IEEE Intl. Symp. on Circuits and Systems (ISCAS)*, 2012.

[9] Y. Chen, G. Parziale, E. Diaz-Santana, and A. K. Jain. 3D touchless fingerprints: Compatibility with legacy rolled images. In *Proc. Intl. Biometric Symposium*, 2006.

[10] H. S. G. Costa, O. R. P. Bellon, L. Silva, and A. K. Bowden. Towards biometric identification using 3D epidermal and dermal fingerprints. In *Proc. Intl. Conf. on Image Processing (ICIP)*, 2016.

[11] L. N. Darlow, S. S. Akhoury, and J. Connan. Internal fingerprint acquisition from optical coherence tomography fingertip scans. In *Proc. Intl. Conf. on Digital Information, Networking, and Wireless Communications (DINWC)*, pages 188–191, 2015.

[12] N. Erdogmus and S. Marcel. Spoofing face recognition with 3D masks. *IEEE Transactions on Information Forensics and Security*, 9:1084–1097, 2014.

[13] A. Fatehpuria, D. L. Lau, and L. G. Hassebrook. Acquiring a 2d rolled equivalent fingerprint image from a non-contact 3d finger scan. In *Proc. SPIE Biometric Technology for Human Identification III (BTHI)*, 2006.

[14] M. S. Khalil and F. Kurniawan. A review of fingerprint preprocessing using a mobile phone. In *Proc. Intl. Conf. on Wavelet Analysis and Pattern Recognition (WAPR)*, 2012.

[15] A. Kumar and C. Kwong. Towards contactless, low-cost and accurate 3D fingerprint identification. In *Proc. Intl. Conf. on Computer Vision and Pattern Recognition (C VPR)*, pages 3438–3443, 2013.

[16] R. D. Labati, A. Genovese, V. Piuri, and F. Scotti. Virtual environment for 3-D synthetic fingerprints. In *Proc. IEEE Int. Conf. on Virtual Environments, Human-Computer Interfaces and Measurement Systems (VECIMS)*, pages 48–53, 2012.

[17] R. D. Labati, A. Genovese, V. Piuri, and F. Scotti. Toward unconstrained fingerprint recognition: a fully-touchless 3-D system based on two views on the move. *IEEE Trans. on Systems, Man, and Cybernetics: Systems*, 46:202–219, 2016.

[18] D. Lee, K. Choi, H. Choi, and J. Kim. Recognizable-image selection for fingerprint recognition with a mobile-device camera. *IEEE Trans. on Systems, Man and Cybernetics - Part B*, 38:233–243, 2008.

[19] X. Lu, D. Colbry, and A. Jain. Matching 2.5D scans for face recognition. In *Proc. of Intl. Conf. on Pattern Recognition (ICPR)*, pages 362–366, 2004.

[20] D. Maltoni, D. Maio, A. K. Jain, and S. Prabhakar, editors. *Handbook of fingerprint recognition*, chapter Fingerprint analysis and representation, pages 97–166. Springer, 2009.

[21] NEC. Nec contactless hybrid fingerprint scanner. Online, 2016. www.nec.com/.

[22] F. Pomerleau, F. Colas, R. Siegwart, and S. Magnenat. Comparing ICP variants on real-world data sets. *Autonomous Robots*, 34:133–148, 2013.

[23] Safran-Morpho. Morphowave scanner. Online, 2016. www.morpho.com/.

[24] A. Sankaran, A. Malhotra, A. Mittal, M. Vatsa, and R. Singh. On smartphone camera based fingerphoto authentication. In *Proc. Intl. Conf. on Biometrics: Theory, Applications and Systems (BTAS)*, 2015.

[25] TBS. TBS 3D-enroll scanner. Online, 2016. www.tbs-biometrics.com/en/.

[26] Y. Wang, Q. Hao, A. Fatehpuria, L. G. Hassebrook, and D. L. Lau. Quality and matching performance analysis of three-dimensional unraveled fingerprints. *Optical Engineering*, 49, 2010.

[27] Y. Wang, L. G. Hassebrook, and D. L. Lau. Data acquisition and processing of 3D fingerprints. *IEEE Trans. on Information Forensics and Security*, 5:750–760, 2010.

[28] B. Yang, X. Li, and C. Bush. Collecting fingerprints for recognition using mobile phone cameras. In *Proc. SPIE Conf. on Multimedia on Mobile Devices*, 2012.

[29] W. Zhou, J. Hu, S. Wang, I. Petersen, and M. Bennamoun. Performance evaluation of a large 3D fingerprint database. *Electronic Letters*, 50:1060–1061, 2014.